Pb-Pb collisions at $\sqrt{s_{NN}} = 2.76$ TeV in a multiphase transport model

Jun Xu[1,*] and Che Ming Ko[2,†]

[1] *Cyclotron Institute, Texas A&M University, College Station, Texas 77843-3366, USA*
[2] *Cyclotron Institute and Department of Physics and Astronomy, Texas A&M University, College Station, Texas 77843-3366, USA*

(Dated: February 16, 2011)

The multiplicity and elliptic flow of charged particles produced in Pb-Pb collisions at center of mass energy $\sqrt{s_{NN}} = 2.76$ TeV from the Large Hadron Collider are studied in a multiphase transport (AMPT) model. With the standard parameters in the HIJING model, which is used as initial conditions for subsequent partonic and hadronic scatterings in the AMPT model, the resulting multiplicity of final charged particles at mid-pseudorapidity is consistent with the experimental data measured by the ALICE Collaboration. This value is, however, increased by about 25% if the final-state partonic and hadronic scatterings are turned off. Because of final-state scatterings, particular those among partons, the final elliptic flow of charged hadrons is also consistent with the ALICE data if a smaller but more isotropic parton scattering cross section than previously used in the AMPT model for describing the charged hadron elliptic flow in heavy ion collisions at the Relativistic Heavy Ion Collider is used. The resulting transverse momentum spectra of charged particles as well as the centrality dependence of their multiplicity density and the elliptic flow are also in reasonable agreement with the ALICE data. Furthermore, the multiplicities, transverse momentum spectra and elliptic flows of identified hadrons such as protons, kaons and pions are predicted.

PACS numbers: 25.75.-q, 12.38.Mh, 24.10.Lx, 24.85.+p

I. INTRODUCTION

Experimental data on Pb-Pb collisions at $\sqrt{s_{NN}} = 2.76$ TeV from the Large Hadron Collider (LHC) by the ALICE Collaboration have recently become available [1–4]. For most central collision bins $(0-5\%)$, the mid-pseudorapidity density of charged particles was found to be $1584 \pm 4(\text{stat.}) \pm 76(\text{sys.})$ [1], which is a factor of 2.2 higher than that observed in central Au-Au collisions at $\sqrt{s_{NN}} = 200$ GeV from the Relativistic Heavy Ion Collider (RHIC). This multiplicity density was reproduced by the HIJING2.0 model with a more modern set of parton distribution functions [5] and has helped to constrain the gluon shadowing parameter in the model [6]. Furthermore, the elliptic flow in non-central collisions was found to have values similar to those in collisions at RHIC energies [2]. According to Ref. [7], the similarity between the elliptic flows at LHC and RHIC is consistent with the predictions of the viscous hydrodynamic model. In Ref. [8], this similarity has further led to the conclusion that the specific viscosity η_s/s of the quark-gluon plasma produced in heavy ion collisions at LHC has a similar value as in heavy ion collisions at RHIC. The observed elliptic flow at LHC can also be described by a kinetic model with a short-lived parton stage but strong final-state hadronic scatterings [9]. As shown in Ref. [10], adding final-state scatterings, which are essential for generating the observed elliptic flow [11], to the HIJING model as implemented in a multiphase transport (AMPT) model [12] would reduce the predicted charged particle multiplicity at mid-rapidity as a result of their appreciable contribution to the longitudinal work [13]. It is thus of interest to study both the multiplicity and elliptic flow in Pb-Pb collisions at $\sqrt{s_{NN}} = 2.76$ TeV by using the AMPT model.

This paper is organized as follows. In Sec. II, we briefly review the AMPT model and discuss its parameters. We then study in Sec. III the multiplicity and in Sec. IV the elliptic flow in Pb-Pb collisions at $\sqrt{s_{NN}} = 2.76$ TeV. Finally, we give some discussions in Sec. V and the conclusions in Sec. VI.

II. THE AMPT MODEL

The AMPT model is a hybrid model with the initial particle distributions generated by the HIJING model [14] of the version 1.383. In the version of string melting, which is used in the present study, hadrons produced from the HIJING model are converted to their valence quarks and antiquarks, and their evolution in time and space is then modeled by the ZPC parton cascade model [15] with the differential scattering cross section

$$\frac{d\sigma}{dt} \approx \frac{9\pi\alpha_s^2}{2(t-\mu^2)^2}. \tag{1}$$

In the above, t is the standard Mandelstam variable for four momentum transfer, α_s is the strong coupling constant, and μ is the screening mass in the partonic matter. After stopping scattering, quarks and antiquarks are converted via a spatial coalescence model to hadrons, which are followed by hadronic scatterings via the ART model [16].

*Electronic address: xujun@comp.tamu.edu
†Electronic address: ko@comp.tamu.edu

In previous studies of heavy ion collisions at RHIC, some of the parameters in the HIJING model were varied in order to reproduce the measured charged particle multiplicity. Specifically, instead of the values $a = 0.5$ and $b = 0.9$ GeV^{-2} used in the HIJING model for the Lund string fragmentation function $f(z) \propto z^{-1}(1-z)^a \exp(-b\, m_\perp^2/z)$, where z is the light-cone momentum fraction of the produced hadron of transverse mass $m_\perp$ with respect to that of the fragmenting string, the values $a = 2.2$ and $b = 0.5$ GeV^{-2} were used in the AMPT model [10]. Also, the values $\alpha_s = 0.47$ and $\mu = 1.8$ or 2.3 fm^{-1}, corresponding to a total parton scattering cross section of 10 or 6 mb, were used for the parton scattering cross section in the AMPT model to describe measured elliptic flow [17, 18] and two-pion correlation functions [19]. In the present study of heavy ion collisions at LHC, we again vary the values of these parameters to fit measured data. As shown below, a reasonable description of the measured charged particle multiplicity density at mid-pseudorapidity is achieved if the default HIJING values of $a = 0.5$ and $b = 0.9$ GeV^{-2} are used in the Lund string fragmentation function. Also, a smaller QCD coupling constant $\alpha_s = 0.33$ and a larger screening mass $\mu = 3.2$ fm^{-1}, corresponding to a smaller (1.5 mb) but more isotropic parton scattering cross section, are needed to reproduce the observed elliptic flow.

III. RAPIDITY DISTRIBUTIONS AND TRANSVERSE MOMENTUM SPECTRA

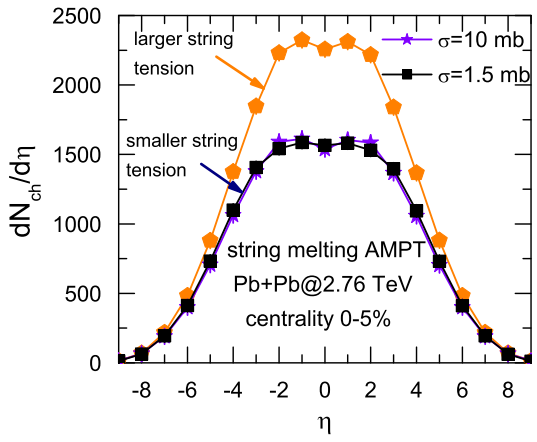

FIG. 1: (Color online) Pseudorapidity distribution of charged particles in Pb-Pb collisions at $\sqrt{s_{NN}} = 2.76$ TeV and centrality of $0-5\%$ from the AMPT model with string melting for larger string tension (filled pentagons) and for smaller string tension with a parton scattering cross section of 10 mb (filled stars) or 1.5 mb (filled squares).

We first show in Fig. 1 the pseudorapidity distribution of charged particles in the most central 5% (b < 3.5 fm) Pb-Pb collisions at $\sqrt{s_{NN}} = 2.76$ TeV from the AMPT model with string melting using different values for the Lund string fragmentation parameters and parton scattering cross sections. It is seen that the values of $a = 2.2$ and $b = 0.5$ GeV^{-2}, that correspond to a larger string tension in the Lund string fragmentation function, gives a larger multiplicity density at mid-pseudorapidity than that from the default HIJING values of $a = 0.5$ and $b = 0.9$ GeV^{-2} that correspond a smaller string tension in the fragmentation function. The multiplicity density is, however, not sensitive to the parton scattering cross section σ. For the smaller value of $\sigma = 1.5$ mb, which is required to reproduce the measured elliptic flow at LHC as shown later in Sec. IV, the resulting charged particle multiplicity of $1,536 \pm 4$ at mid-pseudorapidity obtained with the default HIJING parameters for the string fragmentation function is consistent with the measured data by the ALICE Collaboration. In the following, we will thus use, unless stated otherwise, those parameters that correspond to the smaller values of string tension and parton cross sections in the AMPT model for our study. We note that in obtaining the relation between the centrality c and the impact parameter b, we have used the empirical formula $c = \pi b^2/\sigma_{\rm in}$ [20] with the nucleus-nucleus total inelastic cross section $\sigma_{\rm in} \approx 784$ fm^2 calculated from the Glauber model. Also, we have used in our analysis about $1,000$ AMPT events for the multiplicity density, transverse momentum spectra, and the total elliptic flow, and about $10,000$ events for the transverse momentum dependence of the elliptic flow.

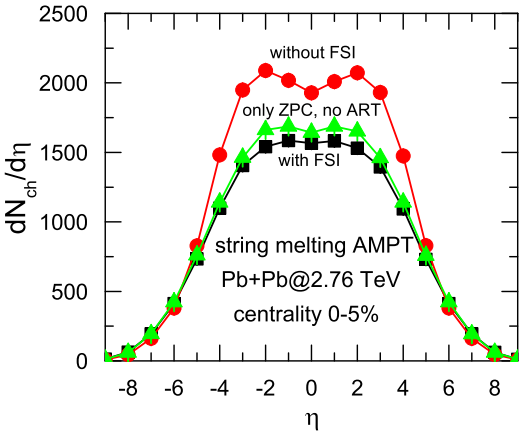

FIG. 2: (Color online) Pseudorapidity distribution of charged particles in Pb-Pb collisions at $\sqrt{s_{NN}} = 2.76$ TeV and centrality of $0-5\%$ from the AMPT model with both final-state partonic and hadronic scatterings (filled squares), with only partonic scatterings (filled triangles), and without final-state interactions (filled circles).

We have also studied the effect of final-state interactions (FSI) on the charged particle multiplicity. As shown by filled circles in Fig. 2, turning off the final-state partonic and hadronic scatterings in the AMPT model enhances the charged particle pseudorapidity distribution.

The charged particle multiplicity at mid-pseudorapidity is now 1925 ± 5, which is essentially the value from the HIJING1.0 model [5] and is about 25% higher than that with the inclusion of final-state scatterings, which is shown by filled squares. The value is reduced to 1642 ± 4 after including partonic scatterings, and this shows that the charged particle pseudorapidity distribution is much more sensitive to partonic than hadronic scatterings.

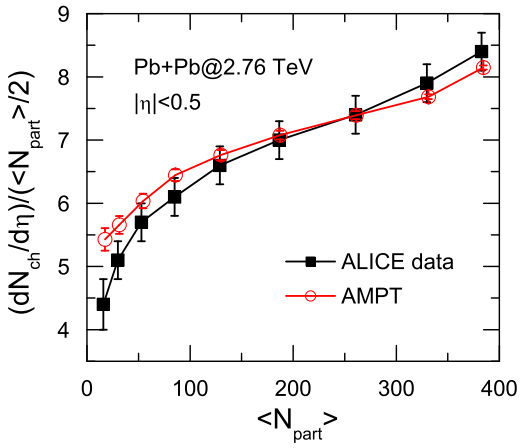

FIG. 3: (Color online) Dependence of charged particle pseudorapidity density per half participant $(dN_{\rm ch}/d\eta)/(\langle N_{\rm part}\rangle/2)$ on the number of participants in Pb-Pb collisions at $\sqrt{s_{NN}} = 2.76$ TeV from the AMPT model with string melting and from the ALICE data [3].

Figure 3 displays the dependence of the charged particle multiplicity density at mid-pseudorapidity ($|\eta| < 0.5$) per 1/2 participant, $(dN_{\rm ch}/d\eta)/(\langle N_{\rm part}\rangle/2)$, on the number of participants. It is seen that results from the AMPT model with string melting (open circles) are roughly consistent with the experimental data, although for peripheral collisions the values are higher than the ALICE data.

For identified hadrons such as protons, kaons, and pions as well as their particles and antiparticles, their rapidity distributions in the $0-5\%$ centrality of same collisions are shown in Fig. 4. The multiplicity ratio of mid-rapidity protons, kaons and pions is roughly $1:2:16$. We note that the multiplicities of each species are again larger if final-state scatterings are not included.

In Fig. 5, the transverse momentum (p_T) spectrum of mid-pseudorapidity ($|\eta| < 0.8$) charged particles (left panel) and those of protons, kaons and pions (right panel) are shown. It is seen that the AMPT model describes reasonably the charged particle p_T spectrum from the ALICE data for small p_T but gives smaller values for large p_T. For identified hadrons, the abundance of pions is the largest at all p_T except at intermediate p_T where the proton yield becomes comparable. A similar phenomenon was observed in heavy ion collisions at RHIC [21], and it was attributed to the enhanced production of baryons from quark coalescence [22–24].

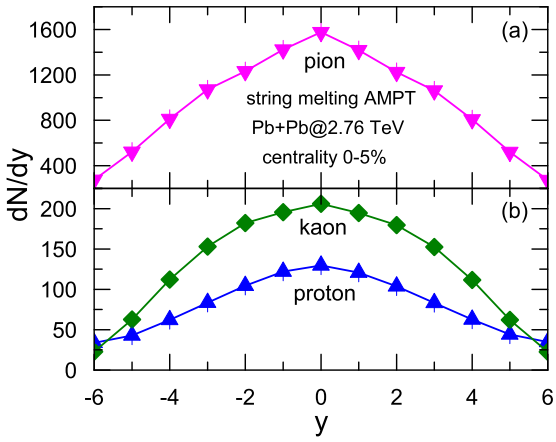

FIG. 4: (Color online) Rapidity distributions of protons, kaons and pions in Pb-Pb collisions at $\sqrt{s_{NN}} = 2.76$ TeV and $0-5\%$ centrality from the AMPT model with string melting.

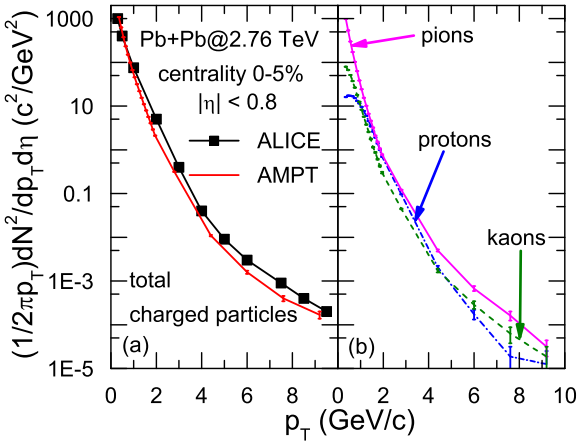

FIG. 5: (Color online) Transverse momentum spectrum of mid-pseudorapidity ($|\eta| < 0.8$) charged particles (left panel) as well as those of protons, kaons, and pions (right panel) in Pb-Pb collisions at $\sqrt{s_{NN}} = 2.76$ TeV and $0-5\%$ centrality from the AMPT model with string melting. Experimental data from the ALICE Collaboration [4] are shown by solid squares in the left panel.

IV. ELLIPTIC FLOWS

In the present study, we determine the elliptic flow using the two-particle cumulant method [25, 26],

$$v_2\{2\} = \sqrt{\langle \cos(2\Delta\phi)\rangle}, \qquad (2)$$

where $\Delta\phi$ is the azimuthal angular difference between particle pairs within the same event and $\langle\cdots\rangle$ means average over all possible pairs. The error of the elliptic flow is calculated by using the method in Ref. [26].

In Fig. 6, we show by filled circles the transverse momentum dependence of the elliptic flow $v_2\{2\}$ of mid-

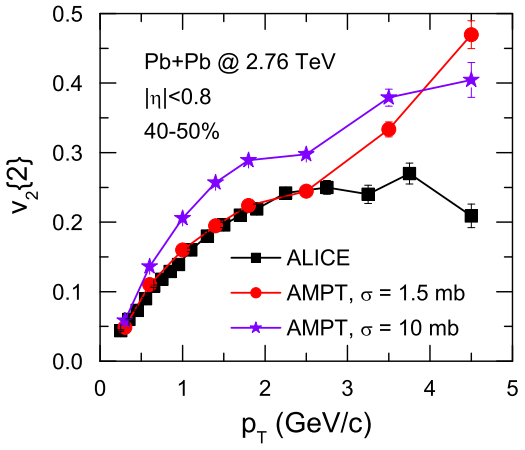

FIG. 6: (Color online) Transverse momentum dependence of the elliptic flow obtained from the two-particle cumulant method for charged particles in Pb-Pb collisions at $\sqrt{s_{NN}} = 2.76$ TeV and $40-50\%$ centrality from the AMPT model with string melting using a parton scattering cross section of 1.5 mb (filled circles) or 10 mb (filled stars). Corresponding experimental data from Ref. [2] are shown by filled squares.

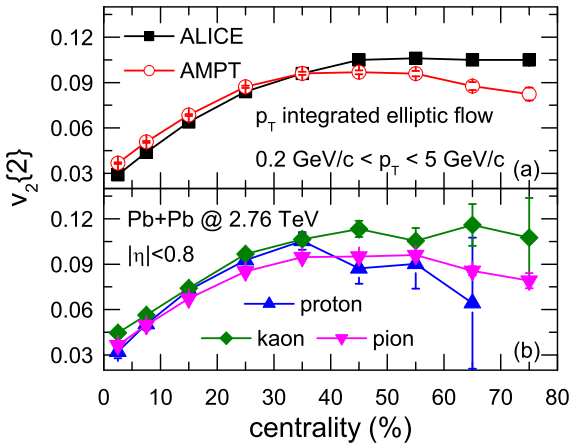

FIG. 7: (Color online) Centrality dependence of the elliptic flow obtained from the two-particle cumulant method for all charged particles (upper panel) and for protons, kaons and pions (lower panel) in Pb-Pb collisions at $\sqrt{s_{NN}} = 2.76$ TeV from the AMPT model with string melting. The ALICE data (filled squares) are from Ref. [2].

pseudorapidity ($|\eta| < 0.8$) charged particles at centrality of $40-50\%$ (10.0 fm < b < 11.2 fm) from the AMPT model and compare it with the ALICE data (filled squares) [2]. It is seen that the elliptic flow from the AMPT model is consistent with the experimental data at $p_T < 2.5$ GeV/c but is larger at $p_T > 2.5$ GeV/c. The latter is likely due to an overestimated non-flow effect in the AMPT model. We note that a satisfactory understanding of elliptic flow of high-p_T particles in heavy ion collisions at RHIC is still lacking [27, 28]. Using the larger parton scattering cross section of 10 mb, corresponding to a larger strong coupling constant ($\alpha_s = 0.47$) and a smaller screening mass ($\mu = 1.8$ fm^{-1}) as used in describing the elliptic flow at RHIC, would lead to a larger elliptic flow (filled stars) than the ALICE data.

The centrality dependence of the $v_2\{2\}$ of mid-pseudorapidity charged particles with transverse momenta 0.2 GeV/c $< p_T <$ 5 GeV/c is shown in the upper panel of Fig. 7 by using again the smaller parton scattering cross section of 1.5 mb. It is seen that the results from the AMPT model (open circles) are consistent with the experimental data (filled squares) except for central and peripheral collisions where they are slightly larger and somewhat smaller, respectively. The smaller elliptic flow for centralities larger than $40-50\%$ is likely related to the softer p_T spectrum in the AMPT model. In the lower panel of Fig. 7, we compare the centrality dependence of the elliptic flows of protons, kaons and pions. Interestingly, the elliptic flow is larger for kaons than for pions.

V. DISCUSSIONS

The above results from the AMPT model for heavy ion collisions at LHC were obtained with different values for the parameters in the Lund string fragmentation function and in the parton scattering cross section from those used for heavy ion collisions at RHIC. The values of $a = 2.2$ and $b = 0.5$ GeV^{-2} used at RHIC for the Lund string fragmentation function correspond to a string tension that is about 7% larger than that for $a = 0.5$ and $b = 0.9$ GeV^{-2} used in the present study. A smaller string tension at LHC is consistent with the fact that the matter formed at LHC is hotter and denser than that at RHIC. The higher temperature reached at LHC also makes it possible to understand, according to the lattice results [29, 30], the smaller QCD coupling constant and the larger screening mass needed to describe the elliptic flow at LHC.

We can compare the property of the quark-gluon plasma produced in heavy ion collisions at LHC with that at RHIC by considering the ratio of its shear viscosity and entropy density, i.e., the specific viscosity. In the kinetic theory, the shear viscosity is given by $\eta_s = 4\langle p\rangle/(15\sigma_{\rm tr})$, where $\langle p\rangle$ is the mean momentum of partons and $\sigma_{\rm tr}$ is the parton transport or viscosity cross section defined by

$$\sigma_{\rm tr} = \int dt \frac{d\sigma}{dt}(1-\cos^2\theta) = \frac{18\pi\alpha_s^2}{E^2}\left[\left(1+\frac{2\mu^2}{E^2}\right)\ln\left(\frac{1+\mu^2/E^2}{\mu^2/E^2}\right)-2\right], \quad (3)$$

where E is the center of mass energy of the colliding parton pair. In obtaining the second line of above equation, we have used Eq. (1). For quark-gluon plasma of

massless quarks and gluons at temperature T, we have $\langle p\rangle = 3T$ and $E \sim \sqrt{18}T$. The entropy density s of the quark-gluon plasma, which is modeled by quarks and antiquarks of current masses in the AMPT, is simply $s = (\epsilon+P)/T = 4\epsilon/(3T) = 96T^3/\pi^2$ if only up and down quarks are considered. The resulting specific viscosity is thus

$$\eta_s/s \approx \frac{3\pi}{40\alpha_s^2}\frac{1}{\left(9+\frac{\mu^2}{T^2}\right)\ln\left(\frac{18+\mu^2/T^2}{\mu^2/T^2}\right)-18}. \qquad (4)$$

The initial temperature of heavy ion collisions in the AMPT model can be estimated from the average energy density of mid-rapidity partons at their average formation time, which is about 46.0 GeV/fm^3 at LHC and 19.5 GeV/fm^3 at RHIC. Using $\epsilon = 72T^4/\pi^2$ for the baryon-free quark and antiquark matter, we obtain an initial temperature of about 468 MeV at LHC and about 378 MeV at RHIC. The value of η_s/s in the early stage of the quark-gluon plasma formed in these collisions, when most of the elliptic flow is generated, is thus about 0.273 at LHC and 0.085 (for $\mu = 1.8$ fm^{-1}) or 0.114 (for $\mu = 2.3$ fm^{-1}) at RHIC.

We note that for fixed values of μ and α_s, which is the case in the AMPT model, the value of η_s/s as given by Eq. (4) increases as the temperature of the quark-gluon plasma decreases. In a more realistic description, the screening mass depends on temperature, i.e., $\mu = gT$ with $g = \sqrt{4\pi\alpha_s}$ [31]. In this case, the ratio η_s/s becomes independent of temperature. It is then of great interest to extend the AMPT model to determine the screening mass from the QCD coupling constant and the local temperature of the partonic matter as in Ref. [32] and use the resulting model to study if using the same QCD coupling constant α_s or same specific viscosity η_s/s in the AMPT model would describe the elliptic flow in heavy ion collisions at both RHIC and LHC, as in the findings of Refs. [7, 8] based on the hydrodynamic model.

VI. CONCLUSIONS

We have used the AMPT model with string melting to study Pb-Pb collisions at center of mass energy $\sqrt{s_{NN}} = 2.76$ TeV. We have found that the measured multiplicity density and elliptic flow of charged particles at mid-pseudorapidity can be reasonably described by the model if the parameters in the Lund fragmentation function are taken to be those used in the default HIJING model and that a smaller but more isotropic parton scattering cross section than that used for heavy ion collisions at RHIC is used. As at RHIC, the final-state partonic and hadronic scatterings were found to be important as they would reduce the charged particle multiplicity density at mid-pseudorapidity by about 25%. The smaller parton cross section needed to describe the measured elliptic flow at LHC than at RHIC has led to a larger estimated η_s/s in the quark-gluon plasma produced at LHC than that at RHIC. However, this result may be due to the use of constant screening mass in calculating the parton scattering cross section. Taking into account the medium dependence of the screening mass may reduce this difference. Furthermore, the transverse momentum spectra and the centrality dependence of the multiplicity and elliptic flow have been studied and they are roughly consistent with the ALICE data. We have also made predictions for the multiplicity distributions and elliptic flows of identified hadrons such as protons, kaons, and pions. Comparisons of these predictions with future experimental data will further enhance our understanding of heavy ion collision dynamics at LHC and the properties of produced quark-gluon plasma.

Acknowledgments

This work was supported in part by the U.S. National Science Foundation under Grant No. PHY-0758115, the US Department of Energy under Contract No. DE-FG02-10ER41682, and the Welch Foundation under Grant No. A-1358.

[1] K. Aamodt, *et al.* (ALICE Collaboration), Phys. Rev. Lett. **105**, 252301 (2010).
[2] K. Aamodt, *et al.* (ALICE Collaboration), Phys. Rev. Lett. **105**, 252302 (2010).
[3] K. Aamodt, *et al.* (ALICE Collaboration), Phys. Rev. Lett. **106**, 032301 (2011).
[4] K. Aamodt, *et al.* (ALICE Collaboration), Phys. Lett. **B696**, 30 (2011).
[5] W.T. Deng, X.N. Wang, and R. Xu, Phys. Rev. C **83**, 014915 (2011).
[6] W.T. Deng, X.N. Wang, and R. Xu, arXiv:1011.5907 [nucl-th].
[7] M. Luzum, arXiv:1011.5173 [nucl-th].
[8] R.A. Lacey, A. Taranenko, N. N. Ajitanand, and J. M. Alexander, arXiv:1011.6328 [nucl-ex].
[9] T.J. Humanic, arXiv:1011.5853 [nucl-th].
[10] Z. W. Lin, S. Pal, C. M. Ko, B. A. Li, and B. Zhang, Phys. Rev. C **64**, 011902(R) (2001).
[11] B. Zhang, C.M. Ko, M. Gyulassy, Phys. Lett. B **455**, 45 (1999).
[12] Z.W. Lin, C.M. Ko, B.A. Li, B. Zhang, and S. Pal, Phys. Rev. C **72**, 064901 (2005).

[13] B. Zhang, C. M. Ko, B. A. Li, and Z. W. Lin, Phys. Rev. C **61**, 067901 (2000).
[14] X.N. Wang and M. Gyulassy, Phys. Rev. D **44**, 3501 (1991).
[15] B. Zhang, Comp. Phys. Comm. **109**, 193 (1998).
[16] B. A. Li and C. M. Ko, Phys. Rev. C **52**, 2037 (1995).
[17] Z. W. Lin and C. M. Ko, Phys. Rev. C **65**, 034904 (2002).
[18] L. W. Chen, C. M. Ko, and Z. W. Lin, Phys. Rev. C **69**, 031901(R) (2004).
[19] Z. W. Lin, C. M. Ko, and S. Pal, Phys. Rev. Lett. **89**, 152301 (2002).
[20] W. Broniowski and W. Florkowski, Phys. Rev. C **65**, 024905 (2002).
[21] K. Adcox *et al.* (PHENIX Collaboration), Phys. Rev. Lett. **88**, 242301 (2002).
[22] R.C. Hwa and C.B. Yang, Phys. Rev. C **67**, 034902 (2003).
[23] V. Greco, C.M. Ko, P. Lévai, Phys. Rev. Lett. **90**, 202302 (2003).
[24] R.J. Fries, B. Müller, and C. Nonaka, S.A. Bass, Phys. Rev. Lett. **90**, 202303 (2003).
[25] S. Wang, Y.Z. Jiang, Y.M. Liu, D. Keane, D. Beavis, S.Y. Chu, S.Y. Fung, M. Vient, C. Hartnack, and H. Stöcker, Phys. Rev. C **44**, 1091 (1991).
[26] N. Borghini, P.M. Dinh and J.Y. Ollitrault, Phys. Rev. C **64**, 054901 (2001).
[27] C. Adler, et al. (STAR Collaboration), Phys. Rev. Lett. **90**, 032301 (2003).
[28] E.V. Shuryak, Phys. Rev. C **66**, 027902 (2002).
[29] O. Kaczmarek and F. Zantow, Phys. Rev. D **71**, 114510 (2005).
[30] O. Kaczmarek, F. Karsch, F. Zantow, and P. Petreczky, Phys. Rev. D **70**, 074505 (2004).
[31] J.P. Blazoit and E. Iancu, Phys. Rep. **359**, 355 (2002).
[32] B. Zhang and W. A. Wortman, Phys. Lett. B **693**, 24 (2010).